Wadi Alshatti University Journal of Pure and Applied Sciences

مجلة جامعة وادي الشاطئ للعلوم البحتة والتطبيقية

Volume 4, No. 2, July-December 2026 Online ISSN: 3006-0877 المجلد 4، الاصدار 2، يوليو- ديسمبر 2026

RESEARCH ARTICLE **SMART MATERIALS**

PZT Piezoelectric Ceramics: A Versatile Material for Quality Monitoring and Structural Integrity Assessment

Abdulhakeem B. Miskeen [1,*], Hala J. El-Khozondar[2], Yasser F. Nassar[1]

[1] Mechanical engineering and renewable energies, Wadi Alshatti University, Brack –Libya
[2] Department of materials and London, centre for nanotechnology, Imperial College London, UK

ARTICLE HISTORY
Received 29 September 2026
Revised 25 October 2026
Accepted 01 November 2026
Online 06 November 2026

KEYWORDS
PZT piezoelectric ceramics;
Acoustic emission;
Weld quality monitoring;
Non-destructive testing;
Structural health monitoring;
defect detection.

ABSTRACT

A PZT-based acoustic emission (AE) sensor was used to record signals during manual arc welding on a mild steel plate. Out of 140 recorded hits, 13 signals from regions of acceptable weld profile were analysed in both time and frequency domains, and the RMS amplitude, peak amplitude, and signal energy were compared between good and defective weld locations. In this limited dataset, all three parameters were consistently higher for poor-quality welds than for the good weld, and this trend was corroborated by metallographic inspection, which confirmed cracks, porosity, and lack of sidewall fusion at the locations of the highest-amplitude signals. Frequency-domain analysis further enhanced the distinction, with defective welds exhibiting peak amplitudes up to 94 dB compared to 60 dB for sound welds. Because the dataset is small and only 13 of 140 recorded hits were analysed, these results should be regarded as an indicative pilot observation rather than a statistically validated finding; they nonetheless illustrate the potential of PZT-based AE sensors for real-time weld-quality monitoring and motivate a larger follow-up study.

السيراميك الكهروضغطي: مادة متعددة الاستخدامات لمراقبة الجودة وتقييم السلامة الهيكلية

عبدالحكيم بشير بن مسكين [1,*]، هالة جارالله اخزندار [2]، ياسر فتحي نصَّار [3]

الكلمات المفتاحية

سيراميك بيزو كهربائي
الانبعاث الصوتي
مراقبة جودة اللحام
الاختبار غير التدميري
مراقبة السلامة الهيكلية
الكشف عن العيوب

الملخص

استُخدم مستشعر للانبعاث الصوتي يعتمد على مادة "PZT" لتسجيل الإشارات أثناء عملية اللحام القوسي اليدوي على لوح من الفولاذ الطري. ومن بين 140 إشارة مسجلة، جرى تحليل 13 إشارة ناتجة عن مناطق ذات مظهر لحام مقبول، وذلك في كل من النطاقين الزمني والترددي؛ حيث تمت مقارنة قيمة RMS للسعة، وسعة الذروة، وطاقة الإشارة بين مواقع اللحام السليمة وتلك التي تعاني من عيوب. وفي هذه المجموعة المحدودة من البيانات، كانت المعايير الثلاثة جميعها أعلى باستمرار في حالات اللحام رديء الجودة مقارنة باللحام السليم. وقد تعزز هذا الاستنتاج من خلال الفحص الميتالوغرافي (المجهري للمعادن)، الذي أكد وجود شقوق ومسامية ونقص في الانصهار عند الجوانب في المواقع التي سُجلت فيها الإشارات ذات السعة الأعلى. كما ساهم التحليل في النطاق الترددي في تعزيز التمييز بين الحالات؛ إذ أظهرت مناطق اللحام المعيبة سعات ذروة وصلت إلى 94 ديسيبل، مقارنة بـ 60 ديسيبل في حالات اللحام السليم. ونظراً لصغر حجم مجموعة البيانات -حيث تم تحليل 13 إشارة فقط من أصل 140- ينبغي اعتبار هذه النتائج ملاحظات أولية استرشادية وليست نتائج مؤكدة إحصائياً. ومع ذلك، فهي توضح الإمكانات الكامنة في مستشعرات الانبعاث الصوتي القائمة على مادة "PZT" لمراقبة جودة اللحام في الوقت الفعلي، مما يشجع على إجراء دراسة أوسع وأكثر شمولاً في المستقبل.

Introduction

Piezoelectric Properties of PZT Ceramics

Lead zirconate titanate (PZT) with the chemical formula $Pb(Zr_xTi_{1-x})O_3$ is a ferroelectric ceramic material that exhibits a strong piezoelectric effect near the morphotropic phase boundary (MPB) at approximately Zr/Ti ratio of 52/48 [1]. The piezoelectric effect allows PZT to convert mechanical stress into electrical charge (sensor mode) and an applied electric field into mechanical strain (actuator mode). This dual behaviour has made PZT a material of choice for sensors, actuators, transducers, and ultrasonic devices[2]. Figure 1 shows a representative PZT-based acoustic emission sensor of the type used in this work.

Acoustic Emission as a Non-Destructive Testing Technique

Non-destructive testing (NDT) techniques are essential in modern manufacturing for verifying product quality and structural integrity without damaging the component under test. Among available NDT methods, acoustic emission (AE) has attracted considerable attention for its ability to detect active defects in real time [3, 4]. Acoustic emission refers to the transient elastic waves generated by the rapid release of energy from localized sources within a material, such as crack growth, plastic deformation, or phase transformation

* Corresponding author
https://doi.org/10.63318/waujpasv4i2_69
This work is licensed under a Creative Commons Attribution-NonCommercial 4.0 International License (CC BY-NC 4.0).

[5] . PZT-based sensors are well suited to AE applications because of their high sensitivity, broad frequency response (typically 100 kHz-1 MHz), and robust performance in harsh industrial environments [6].

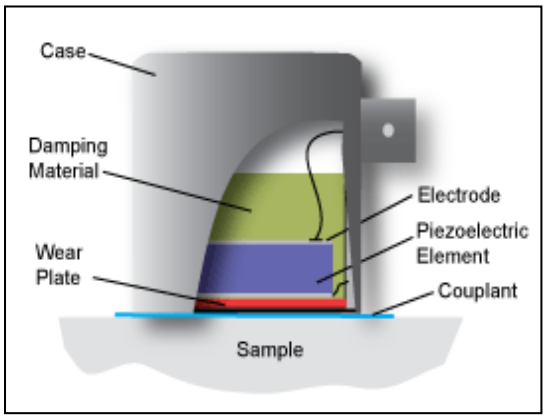


Figure 1. (AE) sensor. Source: www.ndt-*ed.org*

Materials and Methods

Welding is a critical fabrication process used across industries ranging from construction to aerospace, and welding defects can compromise structural integrity and lead to catastrophic failure. Common welding defects include cracks, porosity, slag inclusions, incomplete fusion, lack of penetration, and undercutting [7, 8] Traditional inspection methods, such as radiography and ultrasonic testing, are typically applied post-welding, so defects may already exist by the time they are detected. Online monitoring during welding offers the advantage of enabling immediate corrective action.

Experimental Setup

Following the approach described in a related study on AE-based weld monitoring [9]], a wideband PZT sensor (100 kHz-1 MHz) was mounted on the surface of a mild steel plate (200 x 150 x 5 mm) during manual arc welding. The experimental components are summarised in Table 1, and the schematic layout is shown in Figure 2.

The test specimens were prepared from mild steel plates conforming to AWS standards. Prior to welding, the plates were cut using a plasma cutting machine, followed by milling and surface finishing to ensure uniform surface conditions and eliminate any variations that might affect signal coupling. The weld joint was designed as a single V-groove with a 60° included angle, a 30° bevel angle, and a root gap of 1 mm, as illustrated in Figure 2. A land of 1 mm was also maintained, in accordance with typical practice for butt welding of plates of this thickness.

Welding was carried out manually using an Inverter ES 1600 machine set at 40 A, with E 6013 electrodes of 2.5 mm diameter (AWS A5.1 specification). The welding position was 1G (PA according to ISO 6947). The PZT sensor was securely attached to the plate surface using high-vacuum grease to ensure adequate acoustic coupling, and was positioned away from the direct weld zone to protect it from spatter, as shown in Figure 2. Signals were amplified using a 1220A pre-amplifier with 40 dB gain, and recorded using Physical Acoustic AE-Win 3.1 software with a threshold of 70 dB, a sampling rate of 5 MS/s, and a wavelength setting of 5k. These parameters were determined through trial runs on sample plates of identical dimensions to optimise signal capture.

It is important to clarify that the terms 'good weld' and 'poor weld' in this study refer to specific **regions** along a single welded plate, rather than separate weld specimens. Signals 84 and 93 were identified as representative of sound weld regions, while signals 67, 73, 88, and 97 corresponded to defective regions, as confirmed by subsequent metallographic inspection.

Table 1: Experimental setup

Component	Specification
Material	Mild steel plate (AWS standard)
Electrode	E 6013, 2.5 mm diameter, AWS A5.1 specification
Welding machine	Inverter ES 1600, 40 A
Sensor	Wideband PZT sensor, 100 kHz-1 MHz
Pre-amplifier	1220A, 40 dB gain
Data acquisition	Physical AE-Win 3.1 software + ADC card
Signal analysis	MATLAB software

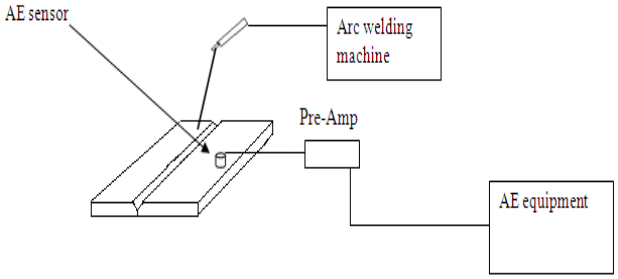


Figure 2: Schematic diagram of the experimental setup [9]

Signal Parameters and Data Analysis

Three parameters were extracted from each AE waveform, x(t), recorded over a hit duration T:

RMS amplitude: $RMS = [\left(\frac{1}{T}\right) \int_0^T x(t)^2 dt]$ the average energy content of the signal.

Peak amplitude: $A_{peak} = max|x(t)|, for\ 0 \leq t \leq T$ the maximum amplitude of a single acoustic event.

Energy: $E = \int_0^T x(t)^2 dt$ the total energy of the signal.

These parameters were computed in MATLAB for each recorded AE hit and used to characterise weld quality (Section 3).

In addition to time-domain analysis, frequency-domain analysis was also performed using MATLAB's Signal Processing Toolbox (sptool) to obtain the peak amplitude in the frequency spectrum for each signal. This was intended to provide an additional layer of characterisation, as certain defects may exhibit distinct frequency signatures. The Fast Fourier Transform (FFT) method was applied to convert the time-domain waveforms into the frequency domain, and the maximum amplitude in the spectrum was recorded for comparison with the time-domain parameters.

It should be noted that although a total of 140 AE hits were recorded during the welding process, only 13 hits were selected for detailed analysis. The remaining hits originated from regions of the weld that exhibited grossly poor profiles, making them unsuitable for meaningful comparison. The selected 13 hits corresponded to areas where the weld bead

was visually acceptable or showed clear indications of potential defects based on preliminary signal screening

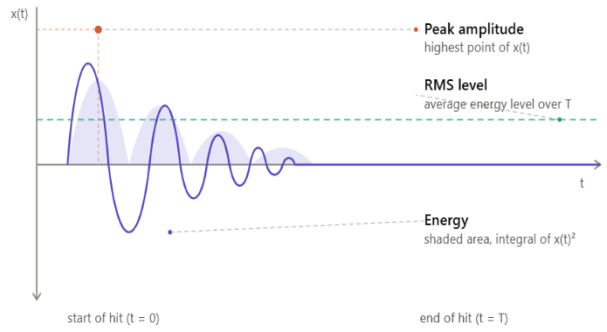


Figure 3 Schematic representation of signal parameters (RMS, peak amplitude, and energy

The selection of these 13 hits was based on two criteria: (i) the weld bead in the corresponding region was visually intact and free from gross macro-defects that would preclude meaningful AE interpretation, and (ii) the signals exhibited clear, distinguishable peaks that could be reliably processed using the automated MATLAB routines. Hits from areas with severe undercutting, excessive spatter, or grossly irregular bead profiles were excluded to avoid contamination of the dataset with artefacts unrelated to the internal weld quality.

Results and Discussion

AE Signal Parameters and Weld Quality

Table 2 summarises the AE signal parameters for all 13 signals that were subjected to detailed analysis. The signals are arranged by their approximate distance from the start of the weld. Signals 84 and 93 were identified as representing the good weld based on their lower parameter values, while signals 67, 73, 88, and 97 exhibited the highest values and were therefore classified as poor welds. The remaining signals (41, 49, 71, 74, 80, 129, 130) showed intermediate values and were associated with minor defects such as lack of penetration or lack of sidewall fusion, as later confirmed by visual inspection.

Table 2: AE signal parameters for good and poor welds

Distance (mm)	Signal	RMS Amplitude (V)	Peak Amplitude (V)	Energy (J)	Peak Freq. (dB)
50-60	41	0.0016	0.0057	5.8642	46.9163
60-70	49	0.0017	0.0081	6.1941	51.2493
70-80	**67**	**0.0028**	**0.0082**	**9.8089**	**94.1144**
80-90	71	0.0016	0.0076	5.8456	47.4451
90-100	**73**	**0.0026**	**0.0082**	**8.5296**	**91.3095**
90-100	74	0.0023	0.0082	8.3775	73.5324
100-110	80	0.0024	0.0082	8.4515	73.6265
100-110	**84**	**0.0020**	**0.0076**	**7.3227**	**59.2074**
110-120	**88**	**0.0027**	**0.0082**	**9.5225**	**84.7154**
110-120	**93**	**0.0022**	**0.0077**	**9.1602**	**60.2916**
120-130	**97**	**0.0026**	**0.0082**	**8.8206**	**78.5553**
160-170	129	0.0019	0.0082	6.5053	55.0955
160-170	130	0.0022	0.0082	7.6794	62.9286

Multiple signals sharing the same distance range (e.g., 73 and 74 at 90-100 mm) originated from the same weld region but were recorded as separate AE hits at slightly different times during the welding process.

When examining the complete dataset, a consistent pattern emerges: the four signals identified as poor welds (67, 73, 88, and 97) exhibit RMS amplitudes ranging from 0.0026 V to 0.0028 V, while the good weld signals (84 and 93) show values of 0.0020 V and 0.0022 V, respectively. This separation, although based on a limited sample, is notable because the two groups occupy distinct ranges without overlap. Similarly, the energy values for the poor welds (8.5296–9.8089 J) are consistently higher than those for the good welds (7.3227–9.1602 J). The peak amplitude in the frequency domain further reinforces this distinction, with poor welds reaching up to 94.1 dB, compared to approximately 60 dB for the good welds.

It is also worth noting that signals 80 and 74, although not classified as the worst, showed elevated parameters relative to the good welds. Visual inspection later confirmed that these signals corresponded to lack of sidewall fusion, which, while not as severe as cracking, still represents a quality concern. This suggests that the AE parameters are not only capable of distinguishing between good and poor welds, but may also offer some degree of gradation in defect severity.

The correspondence between high-amplitude AE signals and metallurgically confirmed defects was particularly clear for signals 67 and 73. Signal 67, which recorded the highest RMS amplitude (0.0028 V), energy (9.8089 J), and frequency-domain peak (94.1 dB), was found to contain a dangerous crack at the 70–80 mm location. Signal 73, with slightly lower values, showed a crack accompanied by porosity at the 90–100 mm region. Signal 88 exhibited a microcrack, while signal 97 was associated primarily with porosity. These findings support the hypothesis that the magnitude of AE parameters is broadly correlated with the severity of the defect, with cracks generating the most energetic emissions and porosity producing intermediate levels.

Key observation: in this pilot dataset, all three AE parameters were higher for poor-quality welds than for the good-quality weld; this trend should be verified with a larger sample.

Defect Detection and Metallographic Confirmation

Table 3 presents the results of the metallographic inspection for the five signals that exhibited the highest AE parameter values. The inspection was performed using an optical microscope at 10× magnification, and the defects were classified according to AWS and API standards, following the procedures used by the Malaysian Institute for Non-Destructive Testing.

Table 3. Metallographic confirmation of defects at high-amplitude AE locations

Signal	Location (mm)	Defect Type	Severity	Additional Observations
67	70-80	Crack	High	Full crack across the weld cross-section
73	90-100	Crack + Porosity	Medium	Small crack accompanied by multiple gas pores
88	110-120	Microcrack	Low	Fine crack visible only under magnification
97	120-130	Porosity	Low	Scattered porosity without cracking
41	50-60	Lack of sidewall fusion	Medium	Large cavity with incomplete fusion

This correspondence between AE signal parameters and metallographically confirmed defects supports the feasibility

of the PZT sensor for real-time defect detection, although, as noted above, confirmation with a larger and independently validated dataset is needed before the method can be considered established for industrial deployment

Advantages of PZT Sensors for Quality Monitoring

Table 4. Summary of PZT sensor properties relevant to quality monitoring [1,2,6]

Property	Advantage for Quality Monitoring
High sensitivity	Detects subtle acoustic emissions from microscopic defects.
Wide frequency range	Captures signals from 100 kHz to 1 MHz, covering most AE phenomena.
Good signal-to-noise ratio	Enables reliable detection in noisy industrial environments.
Fast response	Supports real-time monitoring and immediate feedback.
Durability	Withstands harsh conditions, including high temperature and spatter during welding.
Cost-effectiveness	Relatively low manufacturing cost compared with other advanced sensor types.

Broader Applications of PZT in Quality Monitoring

Beyond weld inspection, PZT-based sensors have been reported in the literature for a range of related applications, summarised in Table 5.

Table 5: Representative applications of PZT-based sensors beyond weld inspection

Application Area	Example Use
Structural health monitoring	Detection of cracks in bridges, buildings, and pipelines.
Fatigue monitoring	Assessment of material degradation under cyclic loading.
Corrosion detection	Monitoring of corrosion-induced damage in metallic structures.
Machine condition monitoring	Detection of bearing faults and machine wear.
Composite materials	Detection of delamination and fibre breakage in composites.
Process control	Monitoring of material behaviour during manufacturing processes.

Limitation

This study has several limitations that should be considered when interpreting the results. First, the case study is restricted to manual arc welding on mild steel plates with a single electrode type; further work is needed to generalise the findings to other welding processes (e.g. MIG, TIG, laser welding) and other materials (e.g. stainless steel, aluminium alloys). Second, the dataset comprises only four weld samples, which limits the statistical robustness of the RMS/peak/energy comparison in Section 3.1; a larger, balanced sample is required to confirm the observed trend. Third, sensor placement and coupling conditions can affect signal amplitude and require standardisation across trials. Finally, the AE parameter thresholds used to flag hits for metallographic inspection were determined empirically for this setup and may not transfer directly to other equipment or welding conditions without recalibration.

Another practical limitation worth mentioning is that out of approximately 140 AE hits recorded during welding, only 13 were deemed suitable for detailed analysis. The majority of the recorded signals originated from regions where the weld profile was excessively poor, making them difficult to interpret reliably in the context of this study. This highlights a challenge inherent to manual arc welding: the process is highly dependent on operator skill, and significant variations in weld quality can occur even within a single pass. As such, the present findings are best viewed as a preliminary demonstration of the technique's potential, rather than a definitive validation

Conclusions

1. PZT-based acoustic emission sensors show promise for online weld-quality monitoring, having detected cracks, porosity, and lack of sidewall fusion in this pilot case study.
2. In the limited dataset examined, RMS amplitude, peak amplitude, and energy were consistently higher for poor-quality welds than for the good-quality weld, though this trend requires confirmation with a larger sample before it can be considered statistically established.
3. Metallographic inspection corroborated the AE-based observations at the locations of the highest-amplitude signals, supporting the plausibility of PZT sensors for defect detection.
4. PZT's broader relevance to structural health monitoring, fatigue assessment, corrosion detection, and other quality-monitoring applications is supported by the wider literature, though this paper does not present new experimental evidence in those areas.
5. Given its sensitivity, durability, and relatively low cost, PZT remains an attractive candidate for industrial NDT applications, pending validation of the present findings on a larger dataset.
6. The inclusion of frequency-domain analysis provided additional discriminatory power, with defective welds exhibiting peak frequency amplitudes up to 94.1 dB compared to approximately 60 dB for sound welds. This suggests that multi-domain (time and frequency) characterisation may enhance the reliability of AE-based weld inspection.

Future Outlook

Building on the preliminary findings above, future work should prioritise: (i) expanding the dataset to a statistically adequate number of welds per quality class; (ii) validating AE-based classification thresholds across multiple welding processes and materials; and, longer term, (iii) exploring automated defect classification using machine learning, wireless/IoT-integrated sensor networks, sensor miniaturisation, and lead-free piezoelectric alternatives.

Author Contributions: Miskeen: Conceptualization, Methodology, mathematical analysis, Writing—original manuscript; **El-Khozondar** and **Nassar**: Editing and review manuscript. Authors have read and agreed to the published version of the manuscript.

Funding: "This research received no external funding."

Data Availability Statement: "No data were used to support this study."
Conflict of Interest: "The authors declare no conflict of interest."
Acknowledgments: "The author would like to express his sincere gratitude to the Department of Mechanical and materials Engineering *Universiti Kebangsaan Malaysia (*UKM) for providing the laboratory facilities and technical support necessary to conduct this research. Special thanks are extended to Prof. Jamaluddin Norddin for his guidance, support and assistance."

References

[1] B. Bera, and M. Sarkar. "Piezoelectric effect, piezotronics and piezophototronics: a review." *Imperial Journal of Interdisciplinary Research (IJIR)*, vol.2, no. 11, pp. 1407-1410, 2016. https://www.academia.edu/37599716/

[2] Z. Zhang, Z. Wang, S. Yang, F. Li, Q. Ke, and A. Physical. "Textured ferroelectric ceramics based 1–3 piezoelectric composite for photoacoustic imaging." *Sensors and Actuators A: Physical*, vol. 380, p. 116030, 2024. https://do.org/ 10.1016/j.sna.2024.116030

[3] H. Kim, et al. "Numerical evaluation of acoustic emission (AE) sensors by lead-zirconate-titanate (PZT) geometric design." Sensors and Actuators A Physical, vol. 366, no, 4, p. 115031, 2024. https://doi.org/10.1016/j.sna.2024.115031.

[4] A. Pollock. "Acoustic emission inspection." in *Nondestructive evaluation of materials*: ASM international, pp. 360-379, 2018.

[5] C. Grosse, M. Ohtsu, D. Aggelis, and T. Shiotani. "Acoustic emission testing: Basics for research–applications in engineering." Springer Nature, 2021. https://link.springer.com/book/10.1007/978-3-030-67936-1

[6] G. Kim, M. Seo, N. Choi, Y. Kim, and K. Kim. "Comparison of PZT, PZT based 1–3 composite and PMN–PT acoustic emission sensors for glass fiber reinforced plastics." *International Journal of Precision Engineering and Manufacturing*, vol. 20, no. 6, pp. 1007-1015, 2019. Htts://doi.org/ 10.1007/s12541-019-00055-7

[7] P. Kah, and J. Martikainen. "Current trends in welding processes and materials: improve in effectiveness." *Reviews on Advanced Materials Science*, vol. 30, no. 2, pp. 189-200, 2012. https://www.researchgate.net/publication/272173827

[8] R. Singh, *Arc welding processes handbook*. John Wiley & Sons, 2021.

[9] A. Miskeen, M. May, and T. Abdullah. "Capability of acoustic emission technique for inspecting manual arc welding defects." *Advanced Materials Research*, vol. 1, no. 1, pp. 2-9, 2017. https://doi.org/ 10.4028/www.scientific.net/AMR.1025-1026.7